RSC Advances

A novel fluorescent pH probe with valuable pKa based on twisted intramolecular charge transfer mechanism, and its applications in cell imaging

Journal:	*RSC Advances*
Manuscript ID:	RA-COM-07-2014-006834.R2
Article Type:	Communication
Date Submitted by the Author:	13-Aug-2014

Complete List of Authors:	Yu, Fang; Sichuan University, College of chemistry Wang, Yan; Chinese Academy of Sciences, Wuhan Institute of Physics and Mathematics Zhu, Wencheng; Sichuan University, National Engineering Research Center for Biomaterials Huang, Yan; Sichuan University, College of Chemistry Ai, Hua; Sichuan University, National Engineering Research Center for Biomaterials; Chinese Academy of Sciences, Wuhan Institute of Physics and Mathematics Yang, Minghui; Chinese Academy of Sciences, Wuhan Institute of Physics and Mathematics Lu, Zhiyun; Sichuan University, College of Chemistry

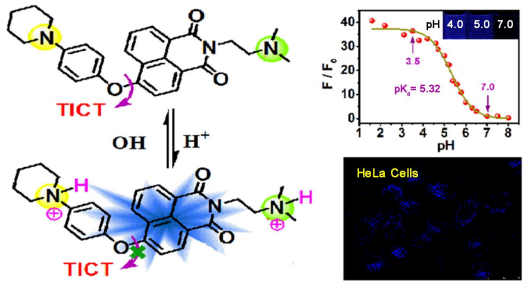

A novel TICT-mechanism based pH probe with valuable pK_a of 5.32 has been developed. It is a promising visualizing agent for lysosomes in intracellular application.

Journal Name

RSCPublishing

COMMUNICATION

A novel fluorescent pH probe with valuable pK_a based on twisted intramolecular charge transfer mechanism, and its applications in cell imaging

Cite this: DOI: 10.1039/x0xx00000x

Fang Yu,[a, ‡] Yan Wang,[b, ‡] Wencheng Zhu,[c] Yan Huang,[a] Minghui Yang,[b,*] Hua Ai[c,*] and Zhiyun Lu[a,*]

Received 00th January 2012,
Accepted 00th January 2012

DOI: 10.1039/x0xx00000x

www.rsc.org/

A novel structurally simple and easily prepared pH probe based on twisted intramolecular charge transfer signaling mechanism, namely Napa-pp has been designed and synthesized. In aqueous buffer solution, it has a valuable pK_a of 5.32 that matches the typical pH range of acidic organelles, hence is applicable for visualizing lysosomes in living cells.

Intracellular pH (pHi) environments (for typical mammalian cells: 4.5-8.0) play a central modulating role in biosystems,[1] since minor variations in pHi may lead to markedly changed cellular behaviors in proliferation, apoptosis, enzymatic activity and ion transport.[2] Accordingly, some illnesses like cancer, stroke and Alzheimer's disease are found to be accompanied with pHi changes.[3] Hence the development of simple and convenient approaches for detecting pHi are of great importance in both cellular analysis and diagnosis.

In comparison with those instrumental analysis methods like H^+-permeable micro-electrode, ^{31}P NMR spectroscopy and optical microscopy for detecting pHi and/or pHi changes,[4] fluorescent pHi chemosensors are more attractive due to their high sensitivity, high specificity, noninvasiveness, and high signal/noise ratio.[5] Furthermore, if the pK_a values of these probes fall in the range of 4.5-8.0 that matches the typical pH environments of biosystems,[6] with the aid of fluorescence microscopic imaging technique, spatial and temporal observation of pHi changes could even be realized.[7]

Based on enormous research efforts, many high performance pH probes have been successfully demonstrated.[8] Yet as far as molecular design strategies are concerned, most of these probes fall into the following three photoluminescence (PL) signalling mechanisms, namely photo-induced electron transfer (PET),[9] intramolecular charge transfer (ICT),[10] and Förster resonance energy transfer (FRET).[11] On the contrary, twisted intramolecular charge transfer (TICT),[12] another well-known mechanism for constructing optical probes,[13] has been less utilized with regard to pH fluorescence chemosensors.[14] Moreover, most of the TICT-based pH probes show relatively low pK_a values of 2.00-4.00,[14a-f] which limit their intracellular applications; while those with valuable pK_as either display UV rather than visible PL emission,[14g] or low sensitivity to pH changes[14h,i]. Consequently, it is still a challenge to construct high performance pHi fluorescent probe based on TICT-mechanism, while the difficulty may lie in the absence of appropriate TICT fluorophores, since two crucial factors should be simultaneously controlled in these luminogens, *i.e.*, the degree of the charge transfer and the change of molecular geometry.[15]

Recently, we have found that if electron-rich carbazolyl groups are introduced into the phenyl (Ph) moiety, the resulting 4-phenyloxy-1,8-naphthalimide derivative (**CzPhONI**) will display strong TICT character.[16] As naphthalimides generally possess high absorption coefficient and good photostability, based on this skeleton, high performance TICT pH sensors might be constructed. In this paper, we report on a quite promising fluorescent pHi probe, namely *N*-(2-(dimethylamino)ethyl)-4-(4-piperidinylphenyloxy)-1,8-naphthalimide (**Napa-pp**, structure shown in Fig. 1), in which a strong electron-donating and proton-acceptable 1-piperidinyl substituent is introduced into the Ph moiety of 4-phenyloxy-1,8-naphthalimide skeleton to endow the molecule with TICT character, while a (2-dimethylamino)ethyl group is connected to the nitrogen atom of the imide group to improve the water solubility of the probe.[9a] The resulted compound **Napa-pp** shows a valuable pK_a of 5.32 that matches the typical pHi range of acidic organelles, and its fluorescence could be "lit up" at pH<7. Hence **Napa-pp** could be applied to visualizing the acidic organelles of living cells.

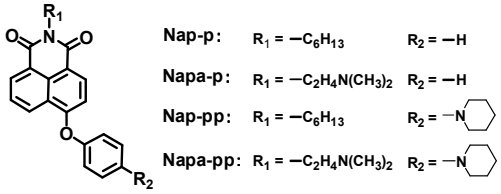

Fig. 1 The four compounds investigated in this article.

To elucidate the TICT fluorescence signalling mechanism of **Napa-pp**, three reference compounds, namely **Nap-p**, **Napa-p** and **Nap-pp** have also been synthesized (structure shown in Fig. 1). In similar solvents, the four compounds show analogous absorption spectra (Fig. 2a), implying that the electronic coupling between naphthalimide (Nap) and Ph units is negligible in their ground states[17]. This deduction is further confirmed by X-ray crystallography characterization results of **Nap-p**[16] and **Napa-pp**, since the Ph and Nap moieties are mutually twisted with large dihedrals of 76.2° and 72.4°, respectively (Fig. S1).

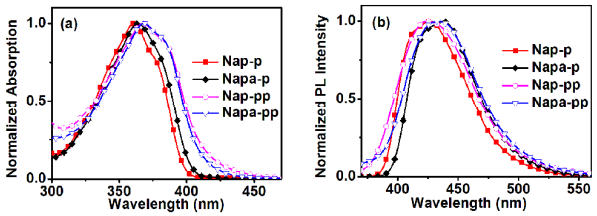

Fig. 2 (a) Absorption; and (b) PL emission spectra (λ_{ex} = 365 nm) of the four compounds in 10.0 μM $CHCl_3$ solution.

Upon photo-excitation, all these four compounds show analogous PL emission spectra in similar solvents (Fig. 2b). However, as illustrated in Table 1 and S2, the four compounds display drastically different PL quantum yields (QYs). In accordance with the literature report,[18] **Nap-p** exhibits high PLQYs (> 0.8) in less polar solvents like toluene (Tol) and CH_2Cl_2, but much dropped fluorescent efficiencies in more polar solvents like MeCN (0.33) and DMSO (0.09). This might be ascribed to either the more advantageous PET process due to the lowered oxidation potentials of the Ph donor moiety in more polar solvents,[19] or the favourable TICT process due to the more stabilized TICT excited states in more polar solvents.[12] In similar solvents, the PLQYs of **Napa-p** are found to be much lower than those of **Nap-p**, indicating that there exists PET process from -$N(Me)_2$ to Nap units in this compound. However, both **Nap-pp** and **Napa-pp** are nearly non-emissive in most solvents, regardless of the solvent polarity (PLQYs < 0.01, vide Table S2). In fact, in Tol, the PLQYs of **Nap-pp** (0.004) and **Napa-pp** (0.001) are even lower than that of **CzPhONI** (0.012), the TICT fluorophore we have reported recently.[16] Taking into account that the electron-donating capability of 1-piperidinyl should be stronger than that of carbazolyl group,[20] the lower PLQYs of **Nap-pp** and **Napa-pp** relative to **CzPhONI** may arise from their stronger TICT character due to the forbidden transition feature of TICT states.[12] Additionally, the more stabilized TICT states of **Nap-pp** and **Napa-pp** should also result in smaller energy gaps that favoring the nonradiative internal conversion process,[21] hence neither dual fluorescence nor positive solvatochromism was observed in these two compounds.

Table 1 Photophysical data of the four napthtalimide derivatives in $CHCl_3$ solution (1.0 μM)

Compd.	λ_{abs} (nm)	λ_{em} (nm)	τ_1(ns)/A_1	τ_2 (ns)/A_2	τ_3 (ns)/A_3	PLQY
Nap-p	361	426	5.80/1.00	-	-	0.810
Napa-p	364	438	5.53/1.00	-	-	0.486
Nap-pp	367	418	0.16/0.14	1.60/0.30	6.04/0.56	0.003
Napa-pp	368	423	0.41/0.17	1.41/0.27	5.74/0.56	0.003

A_n: content of components with different lifetimes;
PLQYs: determined using quinoline sulfate as reference.

Nonetheless, as the low PLQYs of **Nap-pp** and **Napa-pp** may also arise from PET process, to clarify the mechanism, transient PL measurements were performed on these four compounds. As shown in Table 1 and Fig. S2, unlike **Nap-p** and **Napa-p** showing single exponential decays with lifetimes of 5.5~5.8 ns, the fluorescence decays of both **Nap-pp** and **Napa-pp** could only be well-fitted by triexponential functions. Additionally, although both **Nap-pp** and **Napa-pp** display rather low PLQYs, their long-lived excited state species are quite high in content [**Nap-pp**: 6.04 ns (56%); **Napa-pp**: 5.74 ns (56%)]. Consequently, for **Nap-pp** and **Napa-pp**, their excited state components with longer decay lifetimes of 6.04 ns and 5.74 ns could be assigned to the TICT states, validating the TICT mechanism in both **Nap-pp** and **Napa-pp**.[22]

To gain deeper insights into the PL signaling mechanism of **Napa-pp**, its optimized geometries and electronic structures in ground state (S_0) and the first excited state (S_1) in CH_2Cl_2 were calculated with density functional theory (DFT) and time-dependent DFT (TD-DFT) at B3LYP/6-31G (d) level. In accordance with its X-ray crystal structure, the Ph and Nap units of **Napa-pp** are calculated to be nearly orthogonally twisted in S_0 state, and the p orbital of the oxygen atom conjugates more effectively with Nap rather than Ph moiety (Fig. 3a). The HOMO and HOMO-1 are localized on the piperidinylphenyl and (dimethylamino)ethyl units, respectively (Fig. S3), while the LUMO and HOMO-2 are distributed mainly on the Nap moiety. As the electronic transition from S_0 to S_3 states (with composition of HOMO-2→LUMO, vide Table S3) owns the largest oscillator strength, upon photo-excitation, the presence of the two energetically higher HOMO and HOMO-1 orbitals could trigger both PET process from (dimethylamino)ethyl to Nap units and ICT process from piperidinylphenyl to Nap units, leading to fluorescence quenching. Moreover, in the latter case, the HOMO and LUMO of **Napa-pp** in S_1 state are localized on the piperidinylphenyl and Nap units respectively (Fig. 3b); and the optimized geometry of the S_1 state of **Napa-pp** differs significantly from that of the S_0 state, since the twist angle between the Ph unit and the oxygen-linkage plane (φ = C(17)-O(3)-C(7)-C(8)) is 95.07° in S_1 state, but 6.48° in S_0 state (vide Fig. 3b and Table S5). Therefore, the conjugation system in **Napa-pp** would be changed from O-Nap (oxygen conjugates with Nap) in S_0 state to O-Ph (oxygen conjugates with Ph) in S_1 state due to the twisting motion around the two C-O bonds, rationalizing the TICT mechanism.

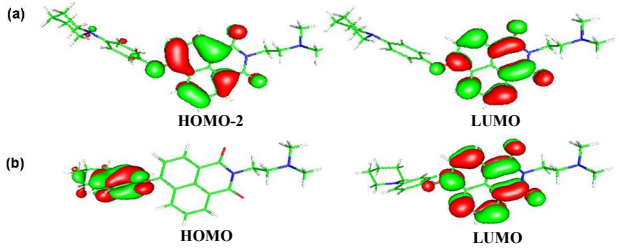

Fig. 3 Optimized geometries and frontier molecular orbitals of **Napa-pp** in (a) the ground state (S_0); and (b) the first excited state (S_1).

On the other hand, for the protonated compound [**Napa-pp** + **2H**$^+$], its HOMO and LUMO are calculated to be distributed dominantly on the Nap moiety in both S_0 and S_1 states (Table S4 and Fig. S4), suggesting that the protonation on **Napa-pp** will prohibit both the PET and TICT processes, leading to fluorescence "light-up". Consistent with these calculation results, ^{1}H NMR measurements indicate that the addition of hydrochloric acid into the DMSO-d_6 solution of **Napa-pp** would trigger distinct downfield-shifted proton signals of both piperidinyl and (dimethylamino)ethyl groups (Fig. S5), verifying that the protonation would occur on the nitrogen atoms of both piperidinyl and -$N(Me)_2$ groups.

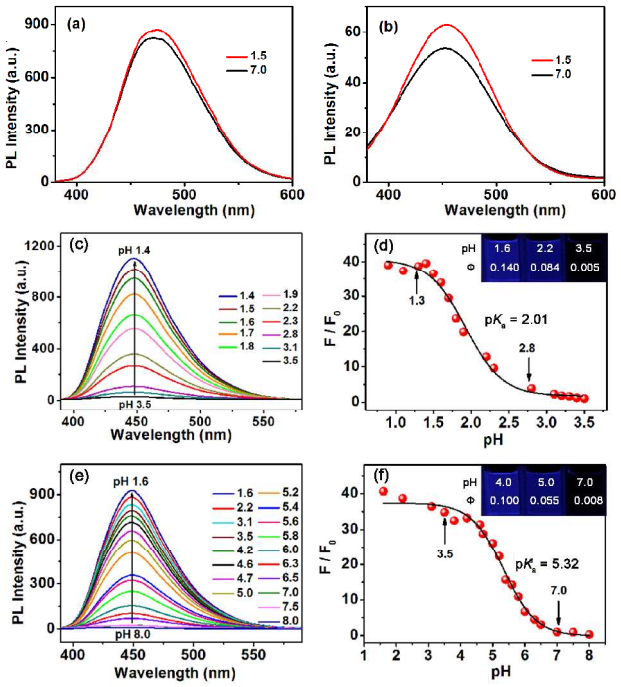

Fig. 4. Fluorescence emission spectra in buffer solutions with different pH values, and the PL emission ratio changes at 450 nm (F/F_0, λ_{ex} = 365 nm) as a function of pH values in DMSO-H_2O (1:250, v/v) buffer solution. (a): **Nap-p** (4.5 μM); (b): **Napa-p** (5.3 μM); (c) and (d): **Nap-pp** (5.3 μM, F_0 is the PL intensity at pH = 3.5); (e) and (f): **Napa-pp** (4.5 μM, F_0 is the PL intensity at pH = 7.0).

The pH titration results of all these four compounds in DMSO-PBS system (1:250, v/v) are illustrated in Fig. 4. **Nap-p** displays negligible PL response toward protons in pH range of 1.5-7.0 (Fig. 4a) due to the lack of suitable proton-binding site. **Napa-p** also shows rather limited PL enhancement upon acidification from pH = 7.0 to 1.5 (Fig. 4b). In fact, even upon addition of excessive hydrochloric acid (0.2 M), the dilute DMSO solution of **Napa-p** displays negligible changes on PL intensity (Fig. S6), indicating that the inhibition of PET effect in **Napa-p** could not trigger a distinct fluorescence "turn-on" response in polar solvents. In sharp contrast to **Nap-p** and **Napa-p**, both **Nap-pp** and **Napa-pp** show obvious PL "switch-on" upon acidification (Fig. 4c, 4e), implying that it should be the inhibition of TICT processes due to the protonation on piperidinyl groups that result in the fluorescence response of **Nap-pp** and **Napa-pp** toward protons. However, the PL emission of **Nap-pp** was found to be "lit up" in acidic environments with pH<3.5, and the PL intensity is enhanced for 39 times when the pH value decreases to 1.4 (Fig. 4d); while the fluorescence of **Napa-pp** could be "switched on" even in neutral environment with pH=7.0, and over 40-fold increased PL intensity could be acquired when pH environment varies from 7.0 to 1.6. According to the pH titration results (Fig. 4d, 4f), in DMSO-PBS buffer system (1:250, v/v), the pK_a values of **Nap-pp** and **Napa-pp** are calculated to be 2.01 and 5.32 (Fig. S7), respectively. Taking into account that the only difference between **Nap-pp** and **Napa-pp** lies in the absence or presence of a PET-charactered (2-dimethylamino)ethyl group, whereas this subunit has no strong electrical relationship with the piperidinylphenyl subunit through either π-conjugation or donor-acceptor interactions, we conjectured that their dissimilar pK_a values might arise from their different solubility in DMSO/H_2O (1/250, v/v) buffer solutions. This hypothesis has been validated through light scattering experiments, since although both **Nap-pp** and **Napa-pp** DMSO-PBS buffer solutions (pH=7.0) are quite transparent, a Tyndall effect could be observed for **Nap-pp** sample (vide Fig. S8), confirming its suspension system nature. When pH titration experiments were conducted in buffer systems with higher DMSO content (DMSO/ H_2O = 1/1, v/v), the PL emission of **Nap-pp** could be "lit up" in environments with pH<5.1, which is less acidic compared to that in buffer system with lower DMSO composition (DMSO/H_2O = 1/250) (pH<3.5), while the fluorescence of **Napa-pp** could be "switched on" in environments with pH<6.1 (Fig. S9). Consequently, the much lower pK_a value of **Nap-pp** relative to **Napa-pp** in nearly aqueous buffer solutions should stem from the low water solubility of **Nap-pp** due to the absence of (2-dimenthylamino)ethyl substituent.

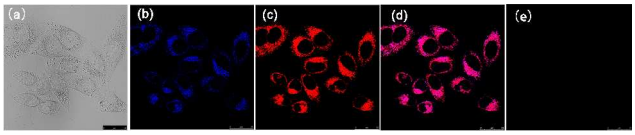

Fig. 5 Confocal fluorescence images of living HeLa cells incubated with different dyes for 0.5 h. (a) The bright field images of HeLa cells; (b) **Napa-pp** (4 μM); (c) **Lyso Tracker** (100 nM); (d) the merge image of (b) and (c); (e) **Napa-pp** (4 μM) for 0.5 h, followed by chloroquine treatment for 0.5 h. The scale bar within the images is 25 μm.

Because in nearly aqueous buffer system, **Napa-pp** shows a valuable pK_a value of 5.32, while the lysosomes of HeLa cell display acidic environments with pH=5.0–6.0,[23] which should be sufficient to activate the PL emission of **Napa-pp**. Furthermore, **Napa-pp** shows low cytotoxicity (Fig. S10), good photostability (Fig. S11), reversible "on-off" fluorescence response toward pH changes (Fig. S12), and satisfactory selectivity toward proton (Fig. S13), thereupon **Napa-pp** may be a promising candidate in intracellular applications. Consequently, confocal fluorescence microscopic imaging experiment was carried on living HeLa cells using **Napa-pp** as fluorescent dye. As expected, punctuated blue fluorescence is discernable in the cytoplasm of **Napa-pp**-incubated samples (Fig. 5b), and further intracellular localization experiments reveal that **Napa-pp** could accumulate in lysosomes of HeLa cells (Fig. 5c, 5d). However, after being treated by chloroquine for 30 min, the fluorescence of **Napa-pp** in HeLa cells was observed to be quenched drastically (Fig. 5e). Therefore, the fluorescence "switch-on" of **Napa-pp** should arise from the protonation on **Napa-pp** in acidic lysosomes of HeLa cells. All these results indicate that **Napa-pp** shows good cell permeability, and could be used to visualize acidic organelles in living cells.

Conclusions

In conclusion, we have developed **Napa-pp** as a structurally simple and easily prepared TICT-mechanism based pH probe. It shows a valuable pK_a of 5.32, which is ideal for investigating the role that H^+ ions play in biological systems. In addition, **Napa-pp** exhibits good photostability, reversible "on-off" fluorescent response toward pH changes, satisfactory selectivity toward proton, good cell permeability, low cytotoxicity, and could localize in lysosomes of HeLa cells. Hence **Napa-pp** is an excellent candidate for visualizing acidic organelles in living cells. Moreover, our results may also shed light on the molecular design strategy for pHi probes based on TICT mechanism.

Acknowledgements

We acknowledge the financial support for this work by National Key Basic Research Program of China (2013CB933903) and the

NSFC (project Nos. 21190031, 21372168, 21373266, 21221064 and 51173117). We also thank Analytical & Testing Center, SCU for providing XRD and NMR data, and the Comprehensive Training Platform of Specialized Laboratory, College of Chemistry, Sichuan University for transient PL measurement.

Notes and references

[a]*Key Laboratory of Green Chemistry and Technology of Ministry of Education, College of Chemistry, Sichuan University, Chengdu, 610064, PR China. E-mail: luzhiyun@scu.edu.cn*
[b]*Key Laboratory of Magnetic Resonance in Biological Systems, State Key Laboratory of Magnetic Resonance and Atomic and Molecular Physics, Wuhan Centre for Magnetic Resonance, Wuhan Institute of Physics and Mathematics, Chinese Academy of Sciences, Wuhan, 430071, PR China. E-mail: yangmh@wipm.ac.cn*
[c]*National Engineering Research Center for Biomaterials, Sichuan University, Chengdu, 610064, PR China. E-mail: huaai@scu.edu.cn*
† Electronic Supplementary Information (ESI) available: Experimental details, X-ray crystallography and spectroscopic property data. See DOI: 10.1039/b000000x/
‡ These authors contributed equally to this work.

1. S. Chen, Y. Hong, Y. Liu, J. Liu, C. W. T. Leung, M. Li, R. T. K. Kwok, E. Zhao, J. W. Y. Lam, Y. Yu, and B. Tang, *J. Am. Chem. Soc*., 2013, **135**, 4926-4929.
2. (a) W. Busa, and R. Nucitelli, *Am. J. Physiol*., 1984, **246**, 409. (b) R. A. Gottlieb, J. Nordberg, E. Skowronski and B. M. Babior, *Proc. Natl. Acad. Sci. U. S. A*., 1996, **93**, 654-658.
3. T. A. Davies, R. E. Fine, R. J. Johnson, C. A. Levesque, W. H. Rathbun, K. F. Seetoo, S. J. Smith, G. Strohmeier, L. Volicer and L. Delva, *Biochem. Biophys. Res. Commun*., 1993, **194**, 537-543.
4. A. Roos and W. F. Boron, *Physiol. Rev*., 1981, **61**, 296-434.
5. (a) J. R. Lakowicz, *Topics in Fluorescence Spectroscopy: Probe Design and Chemical Sensing*; Plenum Press: New York, 1994; Vol. **4**. (b) K. Rurack, *Spectrochim. Acta Part A*, 2001, **57**, 2161-2195.
6. H. J. Kim, C. H. Heo and H. M. Kim, *J. Am. Chem. Soc*., 2013, **135**, 17969-17977.
7. M. Vendrell, D. Zhai, J. C. Er and Y.-T. Chang, *Chem. Rev*., 2012, **112**, 4391-4420.
8. (a) L. Yuan, W. Lin, K. Zheng, L. He and W. Huang, *Chem. Soc. Rev*., 2013, **42**, 622-661. (b) X. Li, X. Gao, W. Shi and H. Ma, *Chem. Rev*., 2014, **114**, 590-659. (c) Z. Guo, S. Park, J. Yoon and I. Shin, *Chem. Soc. Rev*., 2014, **43**, 16-29.
9. (a) J. Xie, Y. Chen, W. Yang, D. Xu and K. Zhang, *J. Photochem. Photobiol. A: Chem*., 2011, **223**, 111-118. (b) D. Aigner, S.M. Borisov, P. Petritsch and I. Klimant, *Chem. Commun*., 2013, **49**, 2139-2141. (c) N. I. Georgiev, A. M. Asiri, A. H. Qustib, K. A. Alamry and V. B. Bojinov, *Sensor. Actuat. B-Chem.,* 2014, **190**, 185-198.
10. (a) X.-D. Liu, Y. Xu, R. Sun, Y.-J. Xu, J.-M. Lu and J.-F. Ge, *Analyst*, 2013, **138**, 6542-6550. (b) J. T. Hutt, J. Jo, A. Olasz, C.-H. Chen, D. Lee and Z. D. Aron, *Org. Lett*., 2012, **14**, 3162-3165.
11. X. Zhou, F. Su, H. Lu, P. Senechal-Willis, Y. Tian, R. H. Johnson, D. R. Meldrum, R. H. Johnson and D. R. Meldrum, *Biomaterials,* 2012, **33**, 171-180.
12. (a) Z. R. Grabowski, K. Rotkiewicz and W. Rettig, *Chem. Rev*., 2003, **10**3, 3899-4031. (b) W. Rettig, *Angew. Chem. Int. Ed*., 1986, **98**, 971-988.
13. J. Wu, W. Liu, J. Ge, H. Zhang and P. Wang, *Chem. Soc. Rev*., 2011, **40**, 3483-3495.
14. (a) S. K. Saha, P. Purkayastha and A. B. Das, *J. Photochem. Photobiol. A: Chem*., 2008, **195**, 368-377; (b) G. Krishnamoorthy, S. K. Dogra, *Chemical Physics*, 1999, **243**, 45-59; (c) M. Sowmiya, A. K. Tiwari, Sonu and S. K. Saha, *J. Photochem. Photobiol. A: Chem*., 2011, **218**, 76-86; (d) G. Jones, J. A.C. Jimenez, *J. Photochem. Photobiol. B: Biol*., 2001, **65**, 5-12; (e) A. Mishra and G. Krishnamoorthy, *Photochem. Photobiol. Sci.,* 2012, **11**, 1356-1367; (f) P. Shen, S. Xiao, X. Zhan, W. Zhang, and K. Chang, *J. Phys. Org. Chem*., 2013, **26**, 858-862; (g) Y. Jiang, *J. Photochem. Photobiol. A: Chem*., 1994, **98**, 205-208; (h) J. Qian, Y. Xu, X. Qian and S. Zhang, *J. Photochem. Photobiol. A: Chem*., 2009, **207**, 181-189; (i) J. Dey and S. K. Dogra , *J. Phys. Chem.*, 1994, **98**, 3638-3644.
15. Q. Li, M. Peng, H. Li, C. Zhong, L. Zhang, X. Cheng, X. Peng, Q. Wang, J. Qin and Z. Li, *Org. Lett*., 2012, **14**, 2094-2097.
16. J. Zhou, P. Chen, X. Wang, Y. Wang, Y. Wang, F. Li, M. Yang, Y. Huang, J. Yu and Z. Lu, *Chem. Commun*., 2014, **50**, 7586-7589.
17. (a) S. Mukherjee, P. Thilagar, *Chem. Commun., 2013,* **49**, 7292-7294; (b) S. Mukherjee, P. Thilagar, Chem. Eur. J. 2014, 20, 8012-8023.
18. N. V. Marinova, N. I. Georgiev and V. B. Bojinov, *J. Photochem. Photobiol. A: Chem*., 2013, **254**, 54-61.
19. H. Sunahara, Y. Urano, H. Kojima, T. Nagano, *J. Am. Chem. Soc*., 2007, **129**, 5597-5604.
20. D. Yang, Q. Y, L. Yang, Q. Luo, Y. Huang, Z. Lu and S. Zhao, *Chem. Commun.,* 2013, **49**, 10465-10467.
21. Y. Yao, J. Xiao, X. Wang, Z. Deng and B. Zhang, *Adv. Funct. Mater*., 2006, **16**, 709-718.
22. (a) M. Kollmannsberger, K. Rurack, U. Resch-Genger and J. Daub, *J. Phys. Chem. A,* 1998, **102**, 10211-10220. (b) D. Kuciauskas, S. Lin , G. R. Seely , A. L. Moore, T. A. Moore and D. Gust, *J. Phys. Chem.*, 1996, **100**, 15926-15932.
23. R. Huang, S.Yan, X. Zheng, F. Luo, M. Deng, B. Fu, Y. Xiao, X. Zhao and X. Zhou, *Analyst,* 2012, **137**, 4418-4420.

